



Effects of azimuthal angle of aeration hole on flows inside and outside an air diffuser pipe

Sato, Ryo
Miyayoshi, Tatsuya
Hayashi, Kosuke
Tomiyama, Akio

(Citation)

Experimental Thermal and Fluid Science, 89:90-97

(Issue Date)

2017-12

(Resource Type)

journal article

(Version)

Accepted Manuscript

(Rights)

© 2017 The Authors. Published by Elsevier Inc.
This is an open access article under the CC BY-NC-ND license
(<http://creativecommons.org/licenses/by-nc-nd/4.0/>).

(URL)

<https://hdl.handle.net/20.500.14094/90005403>



Effects of azimuthal angle of aeration hole on flows inside and outside an air diffuser pipe

Ryo Sato, Tatsuya Miyayoshi, Kosuke Hayashi, Akio Tomiyama*

*Graduate School of Engineering, Kobe University
1-1 Rokkodai, Nada, Kobe 657-8501, Japan*

*corresponding author: tomiyaama@mech.kobe-u.ac.jp

Abstract

Experiments on aeration from a bubble diffuser pipe having five aeration holes are carried out to investigate effects of the azimuthal angle of the holes on flows inside and outside the pipe. The azimuthal angle is varied by rotating the pipe. When the hole angle becomes larger than a certain angle, the liquid height inside the pipe is fixed just below the holes, which results in the prevention of slugging inside the pipe. The effects of hole angle on bubble generation mode and bubble size are small except for the large hole angles, at which generated bubbles are to break up due to an interaction between the bubbles and the pipe wall. Hence uniform aeration is easily realized just by rotating the pipe to some extent. Uniform aeration is also realized with a longer diffuser pipe having ten aeration holes by rotating the pipe. The power in aeration is evaluated from the pressure difference and the total gas inflow. Although the decrease in the hole diameter is also effective to realize the uniform aeration, the increase in the azimuthal angle is superior to the former from the point of view of energy saving.

Keywords: air diffuser pipe; uniform aeration; slugging

Nomenclature

D	pipe diameter (m)
d_H	aeration hole diameter (m)
d	mean diameter of bubbles (m)
E	power in aeration (W)
f_B	bubble frequency (Hz)
g	gravitational acceleration (m/s^2)
h_C	critical liquid height for slugging (m)
h_L	liquid height inside diffuser pipe (m)
Q	gas flow rate (m^3/s)
Q_{IN}	total gas flow rate (m^3/s)
Q_U	ideal flow rate ($= Q_{IN}/5$) (m^3/s)
u	velocity (m/s)
ε	maximum deviation of Q_i
θ	azimuthal angle of hole ($^\circ$)
δ	manometric head (m)
ΔP	pressure difference between duct and exit of aeration hole (Pa)
ρ	density (kg/m^3)

Subscripts

G	gas phase
L	liquid phase
i	aeration hole number

1. Introduction

Aeration has been utilized in various practical applications such as bubble columns and bioreactors in wastewater treatment to enhance mass transfer and liquid mixing [1-3]. Though the desirable aeration state depends on the purpose of applications, many applications prefer uniform aeration [4-7], i.e. uniform distributions of the gas flow rate and bubble size. Various types of gas spargers such as bubble diffuser pipes [4,8], sieve plates [9] and membrane diffusers [10] are available for aeration. Bubble diffuser pipes, which possess multiple aeration holes on their top sides, have often been used in various applications.

Gas-liquid two-phase flows are formed in bubble diffuser pipes in some practical applications. A bubble diffuser pipe in an MBR (membrane bioreactor) [8,11] intendedly introduces liquid into the inside through a bottom opening to prevent blockage of the aeration hole by dried sludge. Fan et al. [12] pointed out that an optimized aeration can be realized at a gas flow rate smaller than a standard operating condition. Aeration at a low gas flow rate is desirable from the point of view of running cost and for formation of mono-dispersed bubbly flows. The decrease in the gas flow rate, however, can also be a possible cause of liquid intrusion.

The authors investigated the relation between the flow inside a diffuser pipe and the uniformity of aeration [8,11]. Figures 1(a) and (b) show examples of the flows inside and outside the pipe, whose dimensions are given in Fig. 1(c). The pipe has five circular holes ($i = 1 - 5$) of $d_H = 5$ mm, where d_H is the hole diameter. Air was flowing from the left side at a constant flow rate, Q_{IN} . $Q_{IN} = 7.0 \times 10^{-4}$ and 3.0×10^{-4} m³/s in Figs. 1(a) and (b), respectively. The pipe was initially filled with water, and then the supplied gas discharged some of the liquid in the pipe and flowed out through the aeration holes as bubbles. The gas and the liquid were separated in the pipe at $Q_{IN} = 7.0 \times 10^{-4}$ m³/s and all the holes always opened for the gas. The distribution of the gas flow rate, Q_i , from each aeration hole was thus uniform as shown in Fig. 2. On the other hand, liquid slugs were formed inside the pipe at $Q_{IN} = 3.0 \times 10^{-4}$ m³/s when the liquid height became larger than a certain critical value. The slug run toward the end of the pipe and disturbed the aeration by covering the aeration hole. The slugging made Q_i non-uniform as shown in Fig. 2. One of the keys to realize uniform aeration even at low Q_{IN} is, therefore, to prevent the slugging by making the liquid height inside the pipe lower than the critical liquid height.

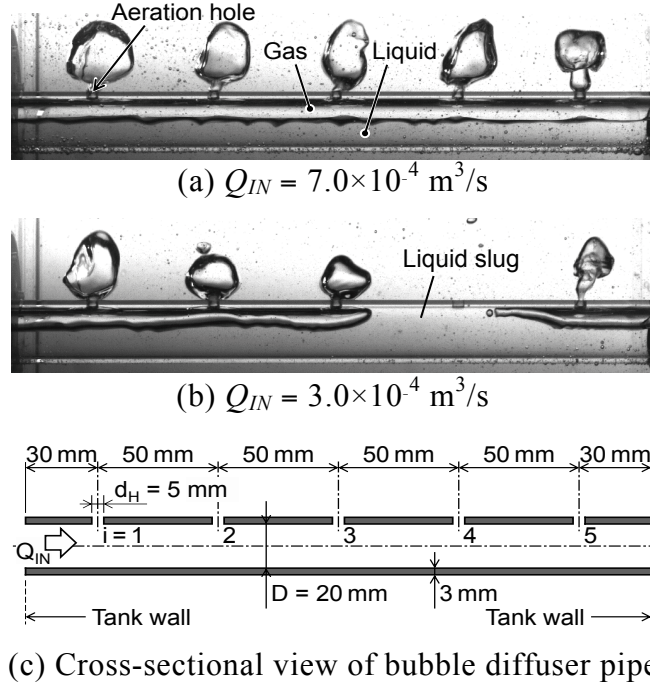


Fig. 1 Flow inside and outside bubble diffuser pipe (D is the pipe diameter.)

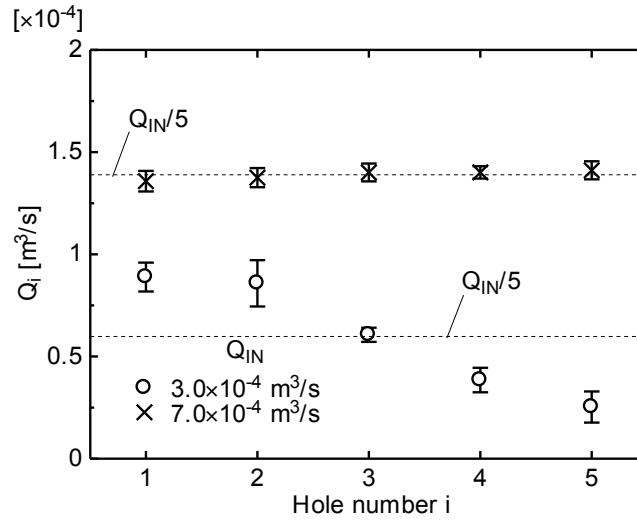


Fig. 2 Distribution of gas flow rate, Q_i , from each aeration hole

The decrease in d_H increases the pressure drop at the aeration hole, which in turn makes the pressure of the gas phase in the pipe higher. It would therefore be a simple way to make the liquid height in the pipe lower by the high pressure. However, from the point of view of the running cost, excess pressure drops should be avoided. We will discuss this point again in Sec. 3.4. One of another possibilities to decrease the liquid height is to change the position of the aeration holes, which may affect the position of

the gas-liquid interface. However there are only a few studies on the uniformity of the gas flow rate from each aeration hole, and our knowledge on the effects of the position of aeration holes on the gas flow rate is rudimentary. In this study, experiments on aeration from the bubble diffuser pipe were therefore carried out to investigate the effects of the hole position by varying the azimuthal angle of the holes. The hole diameter and the diffuser length were also varied to investigate their effects on aeration from the rotated diffuser pipe.

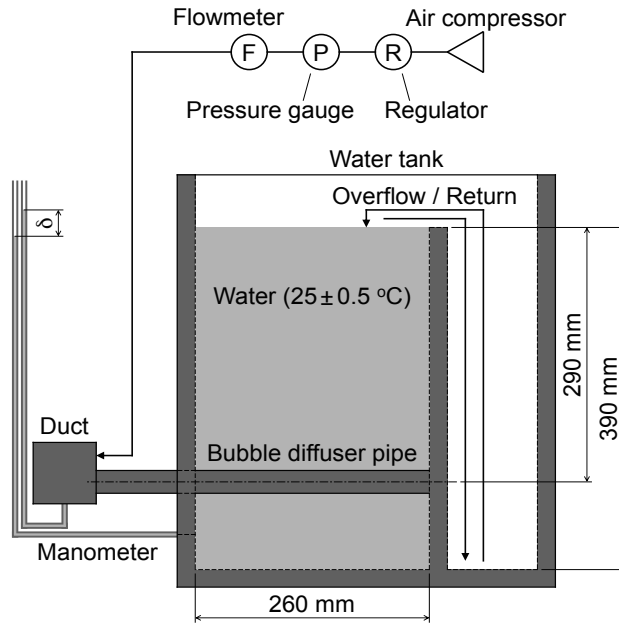
2. Experimental

2.1 Experimental setup and conditions

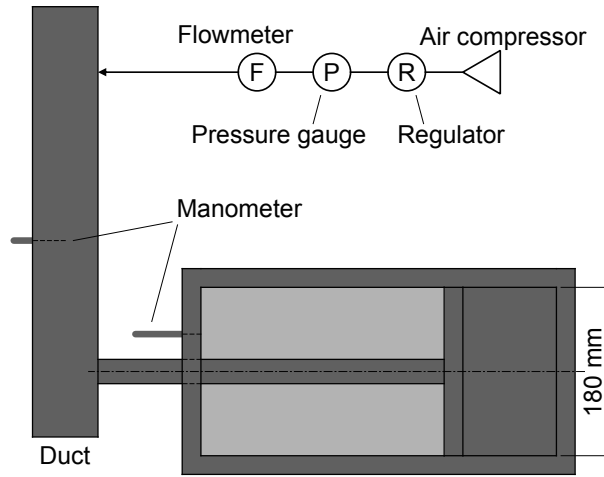
Figure 3 shows the experimental setup. The circular bubble diffuser pipe was horizontally placed in the water tank. A horizontal rectangular duct was connected to the pipe. They were made of transparent acrylic resin for flow visualization. As shown in Fig. 1(c), the inner diameter, length and thickness of the pipe were 20, 260 and 3 mm, respectively. The pipe has five aeration holes. The hole diameter d_H was 5 mm and the spacing between the neighboring holes was 50 mm.

Air at room temperature was used for the gas phase. Tap water was used for the liquid phase and its temperature was kept at 25 ± 0.5 °C. The liquid temperature was measured throughout the experiments using a thermometer (Netsuken, SN3000, accuracy ± 0.1 °C). The tank was filled with the liquid. The elevation of free surface was 390 mm from the bottom of the tank. The distance between the free surface and the pipe axis was 290 mm. Some amount of the liquid overflowed the tank due to burst of bubbles at the free surface and was returned using a pump to keep the elevation of the free surface constant. The gas supplied from the compressor (HITACHI, SRL-2.2DA6) flowed into the pipe through the regulator (Nihon-seiki, BN-3RT5), the flowmeters (Nippon flow cell, SPO-4; Nippon flow cell, STO-4) and the duct. The gas flowed from the left side of the pipe at a constant flow rate and discharged through the holes. The total gas flow rate, Q_{IN} , was varied from 8.0×10^{-5} to 3.0×10^{-4} m³/s.

The azimuthal angle, θ , of the aeration holes was defined as the angle of the hole centers to the vertical axis as shown in Fig. 4. The hole position was changed by increasing θ from 0° to 180° with the interval of 30°. A longer diffuser pipe having ten aeration holes and pipes with $d_H = 1$ and 3 mm were also used to examine the effects of the pipe length and d_H .



(a) Front view



(b) Top view

Fig. 3 Experimental setup

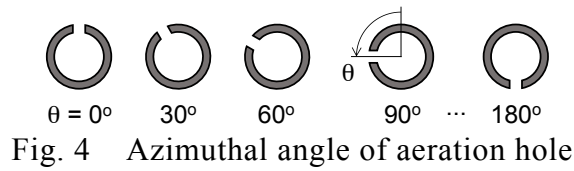


Fig. 4 Azimuthal angle of aeration hole

2.2 Measurement methods

After the flow reached a quasi-steady state, bubbles released from each hole were captured with a graduated cylinder of a certain volume. The gas flow rate, Q_i , from the i th aeration hole was obtained by dividing the cylinder volume by the capturing time.

The measurement was repeated 15 times for each hole to obtain an averaged value. The differences, $|Q_{IN} - \Sigma_{i=1}^5 Q_i|$, were less than 1 % of Q_{IN} under all the conditions. Successive 8-bit grayscale images of flows inside and outside the pipe were taken by using a high-speed video camera (IDT, MotionPro X-3). The shutter speed and the frame rate were 1.9 ms and 300 fps, respectively. The pressure difference, ΔP , between the duct and the aeration hole exit was measured using the manometers as

$$\Delta P = \rho_L g \delta \quad (1)$$

where ρ_L is the density of the water, g is the gravitational acceleration, and δ is the manometric head shown in Fig. 3 (see Appendix for more detail).

3. Results and discussion

3.1 Effects of θ on flow pattern and uniformity of aeration

In this section, discussion will be made mainly on flows at $Q_{IN} = 8.0 \times 10^{-5}$ and $3.0 \times 10^{-4} \text{ m}^3/\text{s}$. Hereafter these flow rates are referred to as Q_{LOW} and Q_{HIGH} , respectively. The flow at Q_{HIGH} and $\theta = 0^\circ$ is shown in Fig. 5(a). A separated flow formed inside the pipe and the gas-liquid interface in the pipe was wavy. Generated bubbles often coalesced with trailing bubbles. The interfacial waves intermittently grew into liquid slugs, which occupied the whole cross section of the pipe. The slugs traveled toward the end of the pipe and covered some aeration holes, which prevented aeration. A similar flow pattern was also observed at $\theta = 30^\circ$ (Fig. 5(b)).

At $\theta = 60^\circ$, the liquid height was fixed just below the aeration holes throughout the experiment as shown in Fig. 5(c). Slugs did not formed at this angle, so that bubbles were continuously generated from all the aeration holes. The liquid height fixing also took place for $\theta > 60^\circ$ as shown in Figs. 5(d)–(g), and all the holes always worked as aeration holes. Especially for $\theta \geq 150^\circ$, the inside of the pipe was almost dry because of the lower position of the hole. The bubbles, however, irregularly broke up due to the interaction between the pipe wall and the bubbles.

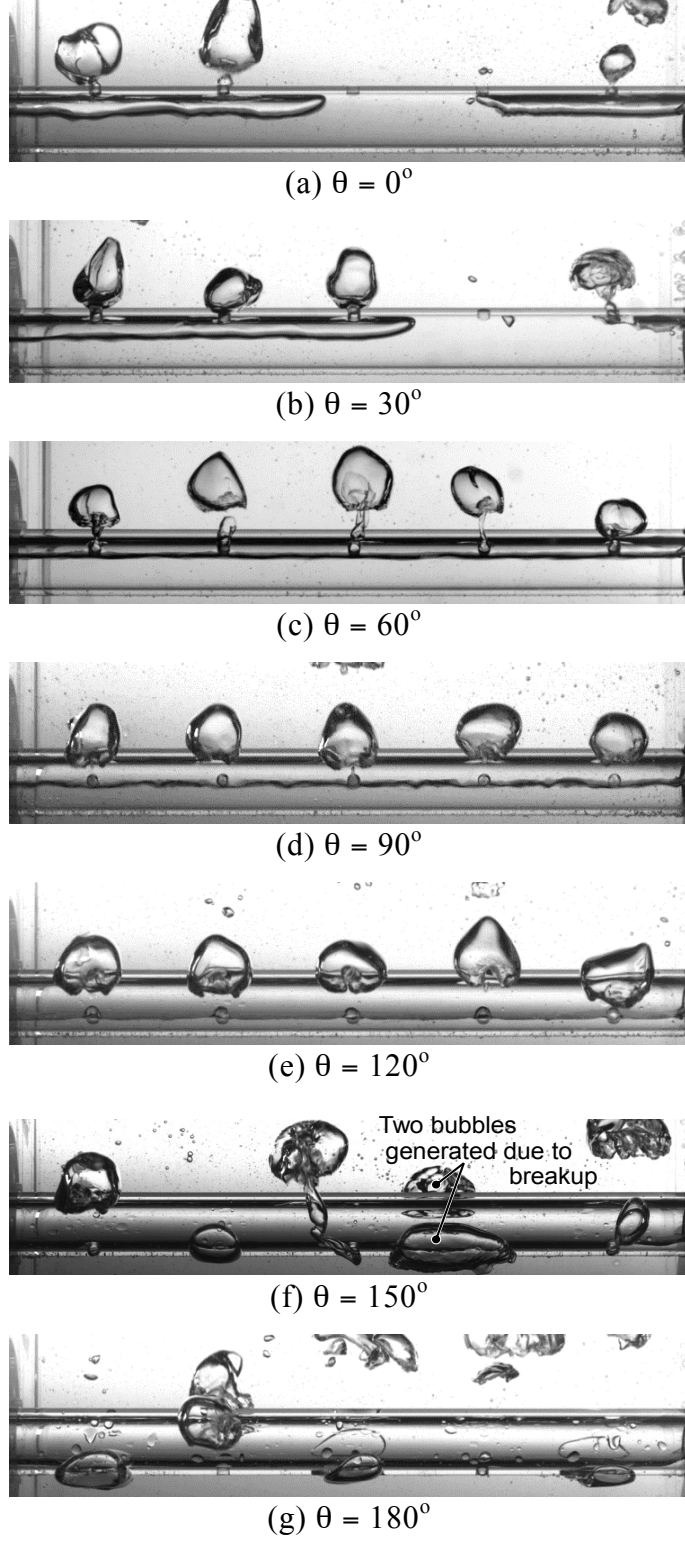


Fig. 5 Flows inside and outside bubble diffuser pipe at Q_{HIGH}

The distributions of Q_i at Q_{HIGH} are shown in Fig. 6. At $\theta = 0^\circ$, the aeration is not uniform, i.e., Q_i decreases with increasing i . This is because the liquid slugs disturbed the aeration [8,11]. The distribution of Q_i at $\theta = 30^\circ$ is also non-uniform. Its

non-uniformity is, however, smaller than that at $\theta = 0^\circ$. The distribution at $\theta = 60^\circ$ is uniform, at which no liquid slugs were formed. Being similar to the distribution of Q_i at $\theta = 60^\circ$, that at $\theta = 90^\circ$ is also uniform since slugging was prevented. The data for $\theta > 90^\circ$ are omitted from the figure since the distributions were almost the same as those at $\theta = 60^\circ$ and 90° . The deviation of Q_i , $(Q_i - Q_U)/Q_U$, from the ideal flow rate Q_U ($= Q_{IN}/5$) corresponding to the perfectly uniform aeration is shown in Fig. 7. The maximum deviation decreases with increasing θ for $\theta \leq 60^\circ$ and becomes constant for $\theta \geq 60^\circ$.

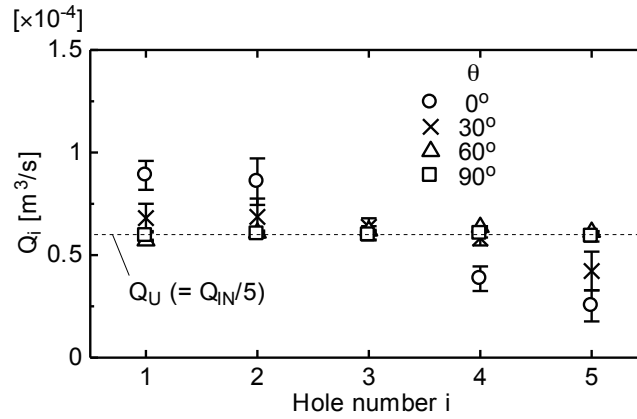


Fig. 6 Effect of θ on distribution of Q_i at Q_{HIGH}

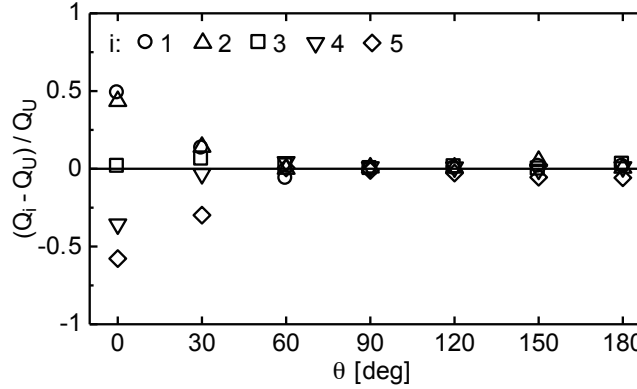


Fig. 7 Deviation of Q_i from Q_U at Q_{HIGH}

In our previous study [8,11], we confirmed that the onset of slugging at $\theta = 0^\circ$ is well predicted by the following Mishima and Ishii's model [13]:

$$u_G - u_L \geq 0.487 \sqrt{\frac{(\rho_L - \rho_G)g(D - h_L)}{\rho_G}} \quad (2)$$

where u_G and u_L are the gas and liquid velocities, ρ_G is the gas density, D is the pipe diameter, and h_L is the liquid height in the pipe. Applying $u_L = 0$ and $\rho_L \gg \rho_G$ to Eq. (2) yields

$$h_L \geq D - 4.22 \frac{\rho_G u_G^2}{\rho_L g} \quad (3)$$

The RHS of this equation represents the critical liquid height, h_C , for slugging. The h_C at $\theta = 30^\circ$ is represented by the white broken lines in Fig. 8(a), in which a wave of $h_L > h_C$ grows into a liquid slug. On the other hand, due to the liquid height fixing, h_L at $\theta = 60^\circ$ was lower than h_C as shown in Fig. 8(b), and no slugs were formed. Thus the liquid height fixing is the key for uniform aeration, and slugging can be easily prevented by setting $\theta \geq 60^\circ$.

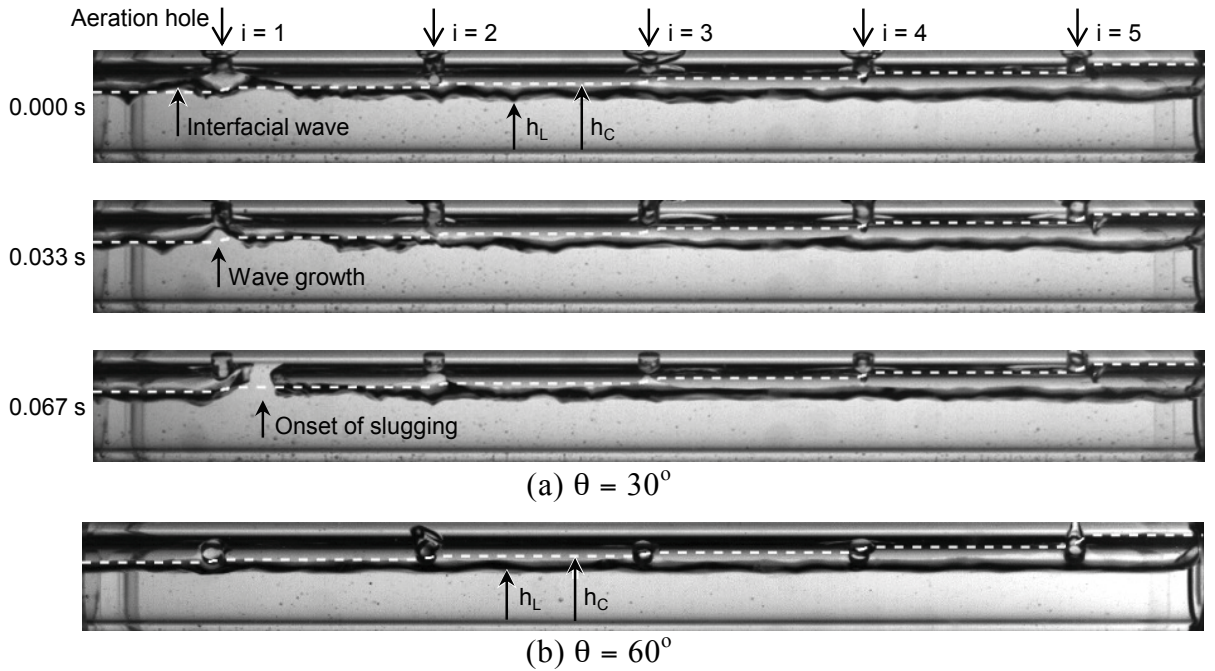


Fig. 8 Critical liquid height and gas-liquid interface at Q_{HIGH}

Flows at Q_{LOW} are shown in Fig. 9. At $\theta = 30^\circ$, the holes of $i = 3, 4$ and 5 were filled with the liquid throughout the experiment. On the other hand, for $\theta \geq 60^\circ$, the gas reached the end of the pipe. The liquid height fixing took place, resulting in no slug

formation and all the holes worked continuously during the aeration. Bubble coalescence was not observed and the bubble release was synchronized for all the holes. The bubbles were smaller than those at Q_{HIGH} . As shown in Fig. 10, the deviation of Q_i at Q_{LOW} for $\theta \leq 30^\circ$ is much larger than that at Q_{HIGH} . However it steeply decreases with increasing θ from 30° to 60° . The effects of θ and Q_{IN} on the maximum deviation

$$\varepsilon = \max_i |(Q_i - Q_U)/Q_U| \quad (4)$$

are summarized in Fig. 11. When $Q_{IN} \leq 3.0 \times 10^{-4} \text{ m}^3/\text{s}$, the deviation is large for $0^\circ \leq \theta \leq 30^\circ$, i.e. the aeration is non-uniform due to the slugging. On the other hand, uniform aeration is realized even in the low Q_{IN} range just by setting θ for $60^\circ \leq \theta \leq 120^\circ$. At higher Q_{IN} ($\geq 5.0 \times 10^{-4} \text{ m}^3/\text{s}$), aeration is uniform for $\theta \leq 120^\circ$. It should be noted that bubbles irregularly break up due to the interaction between the pipe wall and the bubbles for $\theta \geq 150^\circ$ even though ε for $\theta \geq 150^\circ$ are small.

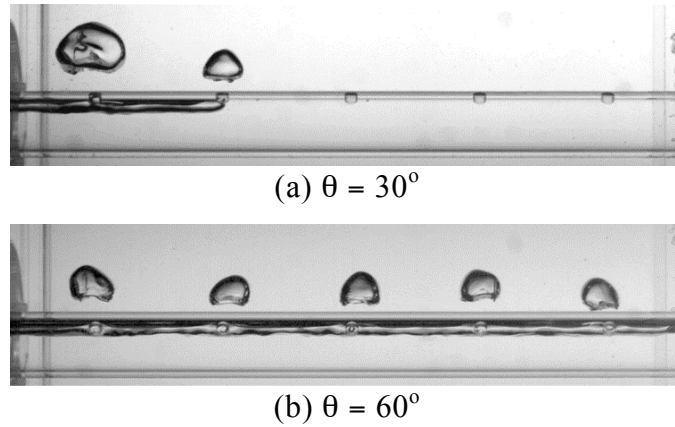


Fig. 9 Flows inside and outside bubble diffuser pipe at Q_{LOW}

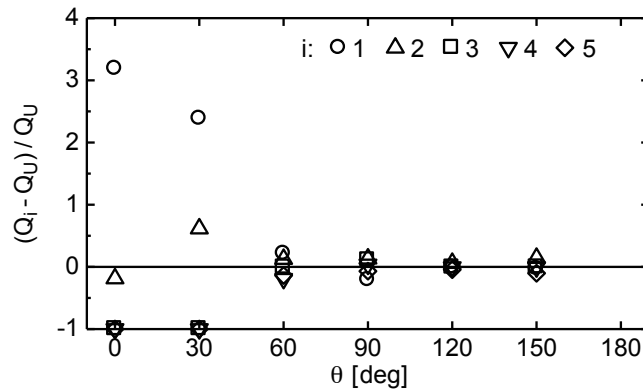


Fig. 10 Deviation of Q_i from Q_U at Q_{LOW}

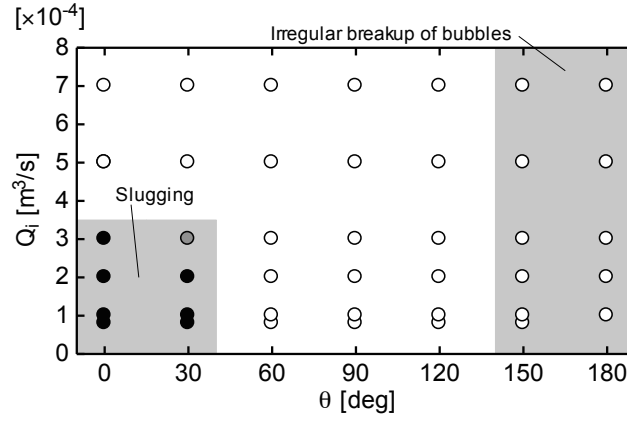
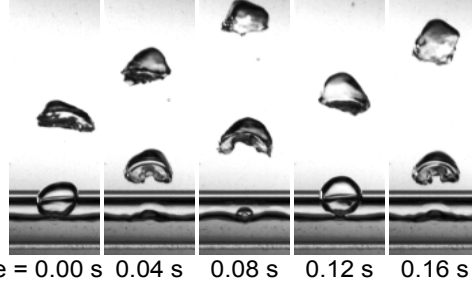


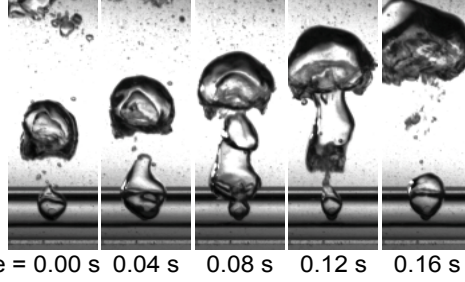
Fig. 11 Effects of θ and Q_{IN} on ϵ (\circ : $\epsilon \leq 0.2$, \bullet : $0.2 < \epsilon \leq 0.5$, \bullet : $\epsilon > 0.5$)

3.2 Bubble diameter

Two bubble generation modes were observed. At Q_{LOW} , single bubbles were formed without bubble coalescence as shown in Fig. 12(a). On the other hand, at Q_{HIGH} , bubbles were generated with coalescence between the leading and trailing bubbles as shown in Fig. 12(b). In the following, these modes are referred to as mode I and II, respectively. Figure 13 shows bubble generation processes at several θ . The bubble generation mode is independent of θ for $\theta \leq 120^\circ$.

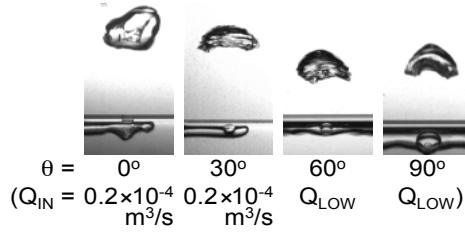


(a) Mode I: Single bubble generation ($\theta = 90^\circ$, Q_{LOW} , $i = 3$)

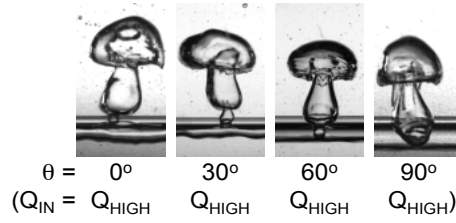


(b) Mode II: Bubble generation with bubble coalescence ($\theta = 90^\circ$, Q_{HIGH} , $i = 3$)

Fig. 12 Bubble generation modes



(a) Mode I ($Q_i = 0.2 \times 10^{-4} \text{ m}^3/\text{s}$)



(b) Mode II ($Q_i = 0.6 \times 10^{-4} \text{ m}^3/\text{s}$)

Fig. 13 Effects of θ and Q_i on bubble generation mode

The mean diameter, d_i , of bubbles generated from the i th hole was evaluated as

$$d_i = \sqrt[3]{\frac{6 Q_i}{\pi f_{Bi}}} \quad (5)$$

where f_{Bi} is the bubble frequency measured by counting the number of bubbles passing

through the elevation 50 mm above the top of the pipe using the high-speed video images for ten seconds. It should be noted that, in mode II, bubbles at this elevation were formed by coalescence of two or three bubbles. For modes I and II, the distributions of d_i were uniform except for the cases, in which Q_i were non-uniform e.g., $(Q_{IN}, \theta) = (Q_{LOW}, 0^\circ)$ and $(Q_{HIGH}, 0^\circ)$ as shown in Fig. 14.

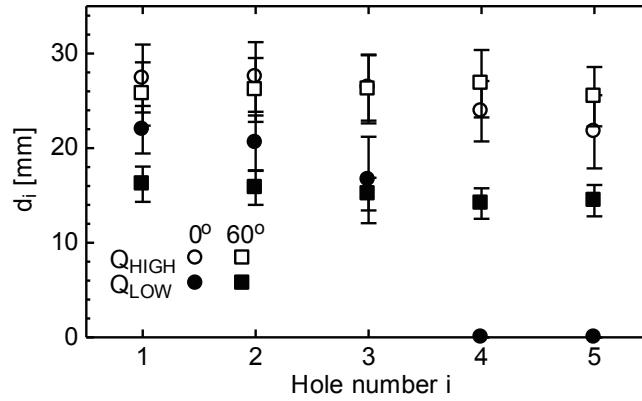


Fig. 14 Effect of θ on distribution of d_i

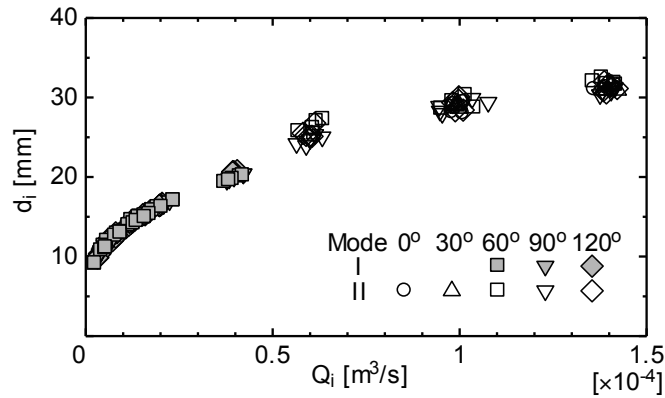


Fig. 15 d_i plotted against Q_i

Figure 15 shows d_i plotted against Q_i . The data for non-uniform aeration and for $\theta = 150^\circ$ and 180° with irregular breakup of bubbles were omitted. The diameter monotonously increased with increasing Q_i . In spite of the difference in θ , the data lie on a single curve. Hence the effect of θ on the mean bubble diameter is small, and therefore, the rotation of the diffuser pipe realizes uniform distributions not only of Q_i but also of d_i . It should, however, be noted that the use of $\theta \geq 150^\circ$ causing irregular bubble breakup is not recommended.

3.3 Long diffuser pipe

Flows inside and outside a longer bubble diffuser pipe (510 mm in length) having ten aeration holes are shown in Fig. 16. The hole diameters and the pipe diameter were 5 and 20 mm, respectively. The pipe length and Q_{IN} were twice as large as those in the case in Fig. 5. At $\theta = 0^\circ$, liquid slugs were formed. In addition, the gas did not reach the end of the pipe. The distribution of Q_i was non-uniform as shown in Fig. 17. On the other hand, at $\theta = 90^\circ$, the liquid height was fixed to the holes and the distribution of Q_i became uniform. Increasing θ is thus very effective to easily realize uniform aeration.

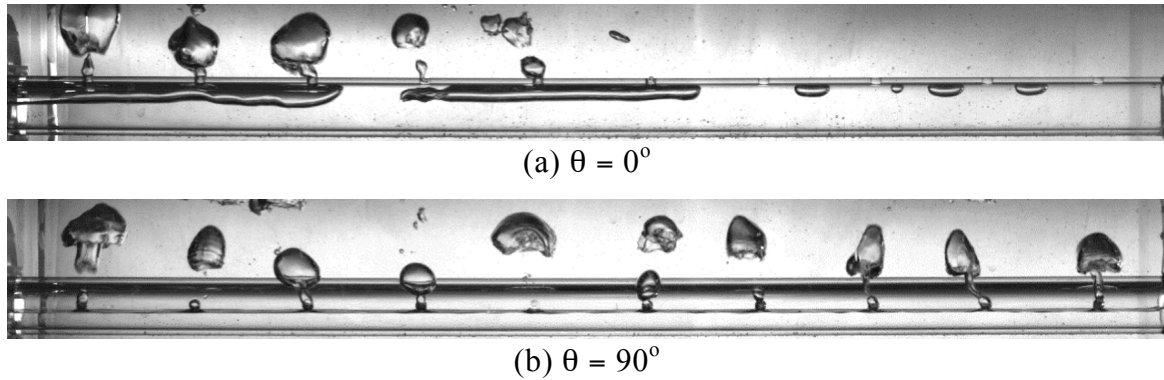


Fig. 16 Flows inside and outside diffuser pipe with ten aeration holes at $Q_{IN} = 6.0 \times 10^{-4} \text{ m}^3/\text{s}$ ($= 2 Q_{HIGH}$)

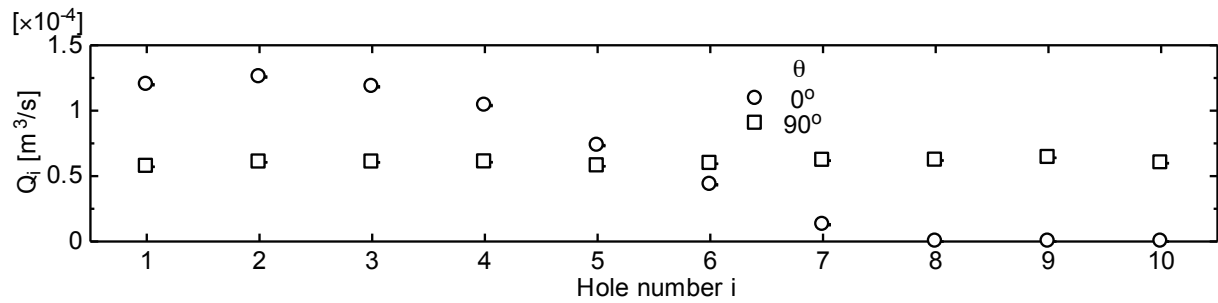


Fig. 17 Effect of θ on distribution of Q_i at diffuser pipe with ten aeration holes at $Q_{IN} = 6.0 \times 10^{-4} \text{ m}^3/\text{s}$

3.4 Effect of d_H

Figure 18 shows flows inside and outside a diffuser pipe with holes of $d_H = 3 \text{ mm}$ and Q_{LOW} . As in the case of 5 mm hole, liquid slugs were formed at $\theta = 0^\circ$ (Fig. 18(a)) and 30° . For $\theta \geq 60^\circ$, the liquid height was fixed to the holes, and therefore, slugging was prevented as shown in Fig. 18(b). The gas flow rate also became uniform just by rotating

the pipe as shown in Fig. 19.

The flow at $d_H = 1$ mm, Q_{LOW} and $\theta = 0^\circ$ is shown in Fig. 20. In spite of small θ , the gas reached the end of the pipe and no slugs were formed inside the pipe. As shown in Fig. 21, the deviation of Q_i is small even at small θ , and θ has no influence on the uniformity. However generated bubbles tended to coalesce with some trailing bubbles.

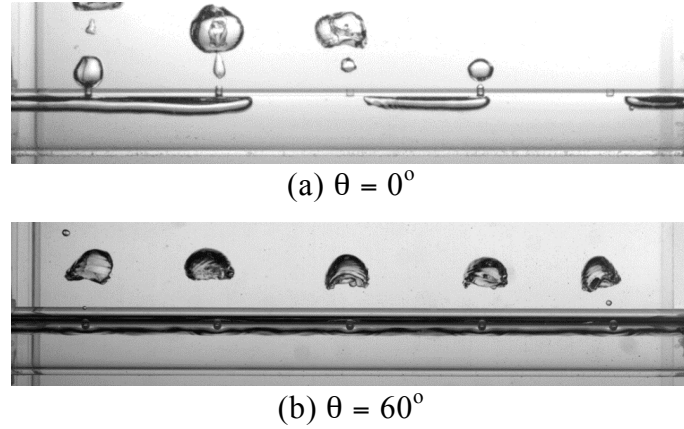


Fig. 18 Flows inside and outside diffuser pipe at $d_H = 3$ mm and Q_{LOW}

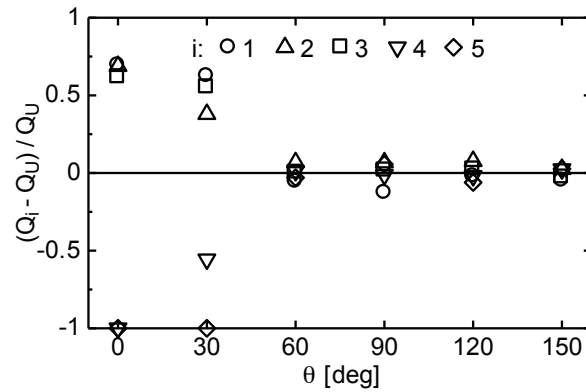


Fig. 19 Deviation of Q_i from Q_U at $d_H = 3$ mm and Q_{LOW}

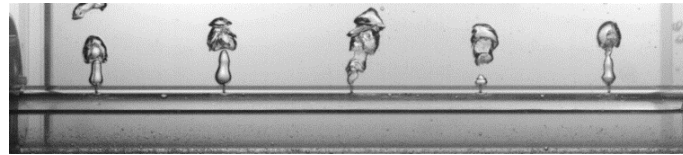


Fig. 20 Flows inside and outside bubble diffuser pipe at $d_H = 1$ mm, Q_{LOW} and $\theta = 0^\circ$

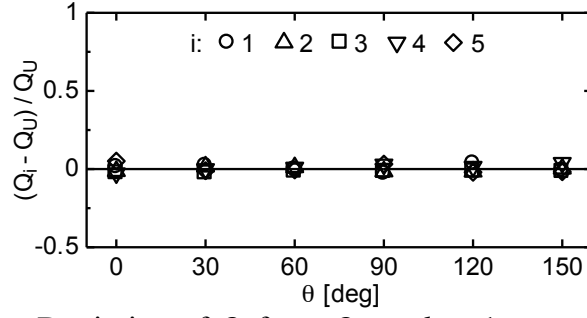


Fig. 21 Deviation of Q_i from Q_U at $d_H = 1$ mm and Q_{LOW}

The power, E , in aeration was evaluated as

$$E = \Delta P Q_{IN} \quad (6)$$

The effects of d_H and Q_{IN} on ΔP and E in the case of $\theta = 60^\circ$, at which the gas flow rate was uniform at all d_H , are shown in Fig. 22. The decrease in d_H makes E significantly larger. The increase in θ is, therefore, superior to the decrease in d_H from the point of view of energy saving.

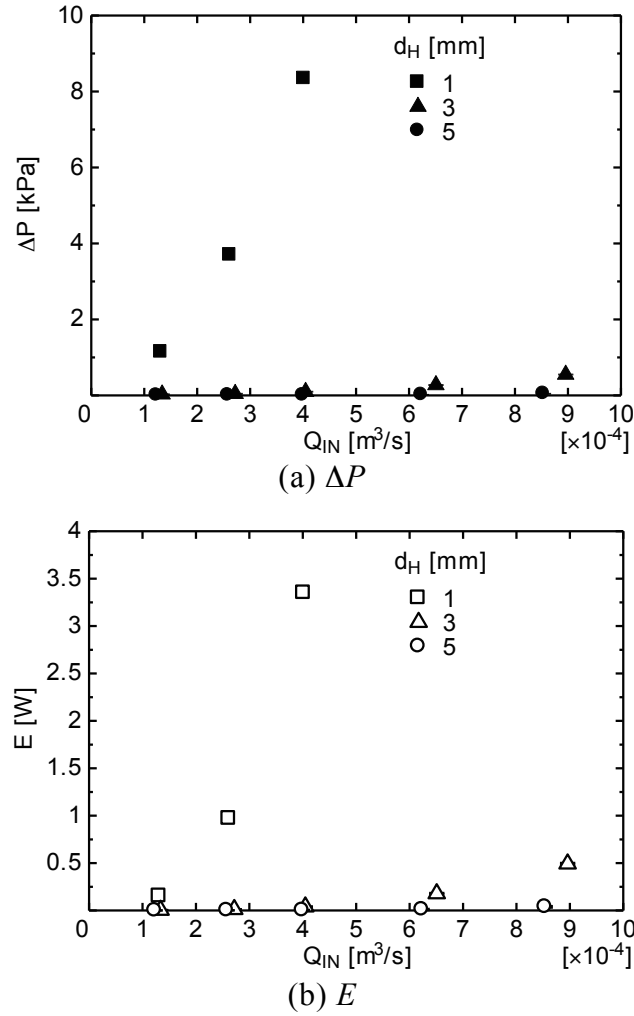


Fig. 22 Effects of d_H and Q_{IN} on ΔP and E

4. Summary and conclusions

Experiments on aeration from a bubble diffuser pipe having multiple aeration holes were carried out to investigate effects of the azimuthal position of the holes on the flows inside and outside the pipe. The pipe diameter was 20 mm. The hole diameters were 5 mm. The azimuthal angle θ was varied from 0 to 180°. The gas and liquid phases were air and water, respectively. The total gas flow rate was varied from 8.0×10^{-5} to $3.0 \times 10^{-4} m^3/s$. The flows inside and outside the pipe were observed using a high-speed video camera. The gas flow rates, Q_i , from each hole were measured by capturing generated bubbles. A map for the uniformity of Q_i in terms of the total gas flow rate and θ was presented. The mean diameter, d_i , of bubbles was evaluated from Q_i and the bubble frequency. The effects of θ for a longer bubble diffuser pipe and for smaller d_H , i.e. $d_H = 1$ and 3 mm, were also investigated. The conclusions obtained under the present experimental conditions are as follows:

- (1) When θ becomes larger than a certain angle, the maximum liquid height inside the pipe is fixed just below the holes, which results in the prevention of slugging.
- (2) Uniform aeration is easily realized just by setting $\theta \geq 60^\circ$ due to the liquid height fixing.
- (3) The mean diameter of bubbles generated from each hole is uniform when Q_i is uniform. The effect of θ on the bubble size is small except for $\theta \geq 150^\circ$ for which bubbles irregularly break up due to the interaction between the pipe wall and the bubbles.
- (4) Increasing θ is a better way to realize uniform aeration than decreasing d_H from the point of view of energy saving.

Appendix

The pressure difference, ΔP , between the pressure in the duct, P_G , and that at the aeration hole exit, P_e , was measured using the manometer as shown in Fig. A1. Hereafter the liquid columns of the manometer attached to the duct and the tank are referred to as column (a) and (b), respectively. The manometric head, δ , for the two manometer liquid columns is given by

$$\delta = (h_a - h_a') - (h_b - h_b') \quad (\text{A1})$$

where h_a and h_b are the liquid heights in column (a) and (b), and h_a' and h_b' are the distances from the gas-liquid interface inside the pipe to the bottom levels of columns (a) and (b), respectively. The pressures P_G and P_e are given by

$$P_G = \rho_L g(h_a - h_a') + P_\infty \quad (\text{A2})$$

$$P_e = \rho_L g(h_b - h_b') + P_\infty \quad (\text{A3})$$

where P_∞ is the atmospheric pressure. Hence the pressure difference $\Delta P = P_G - P_e$ is given by Eq. (1), i.e. $\Delta P = \rho_L g \delta$.

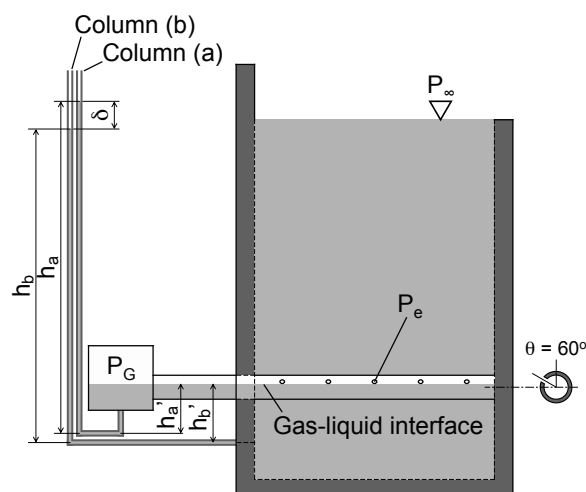


Fig. A1 Measurement method of pressure difference

Acknowledgement

This work has been supported by JSPS KAKENHI Grant Number 15H03920.

References

- [1] K. I. Ashley, D. S. Mavinic and K. J. Hall, Bench-scale study of oxygen transfer in coarse bubble diffused aeration, *Water Research*, 26(10), pp. 1289-1295, 1992.
- [2] A. Ng and A. Kim, A mini-review of modelling studies on membrane bioreactor (MBR) treatment for municipal wastewaters, *Desalination*, 212, pp. 261-281, 2007.
- [3] P. Rollbusch, M. Bothe, M. Becker, M. Ludwig, M. Grunewald, M. Schluter and R. Franke, Bubble columns operated under industrially relevant conditions - Current understanding of design parameters, *Chemical Engineering Science*, 126, pp. 660-678, 2015.
- [4] A. Sofia, W. J. Ng and S. L. Ong, Engineering design approaches for minimum fouling in submerged MBR, *Desalination*, 160, pp. 67-74, 2004.
- [5] N. Kantarci, F. Borak and K. O. Ulgen, Bubble column reactors, *Process Biochemistry*, 40, pp. 2263-2283, 2005.
- [6] A. A. Kulkarni and J. B. Joshi, Bubble formation and bubble rise velocity in gas-liquid systems: a review, *Industrial & Engineering Chemistry Research*, 44, pp. 5873-5931, 2005.
- [7] D. D. McClure, C. Wang, J. M. Kavanagh, D. F. Fletcher, G. W. Barton, Experimental investigation into the impact of sparger design on bubble columns at high superficial velocities, *Chemical Engineering Research and Design*, 106, pp. 205-213, 2016.

- [8] R. Sato, K. Hayashi and A. Tomiyama, Effects of liquid viscosity on flows inside and outside a bubble diffuser pipe, *Experimental Thermal and Fluid Science*, 66, pp. 197-205, 2015.
- [9] N. A. Kazakis, I. D. Papadopoulos and A. A. Mouza, Bubble columns with fine pore sparger operating in the pseudo-homogeneous regime: gas hold up prediction and a criterion for the transition to the heterogeneous regime, *Chemical Engineering Science*, 62, pp. 3092-3103, 2007.
- [10] P. Painmanakul, K. Loubiere, G. Hebrard and P. Buffiere, Study of different membrane spargers used in waste water treatment: characterization and performance, *Chemical Engineering and Processing*, 43, pp. 1347-1359, 2004.
- [11] F. Kira, S. Furuno, K. Hayashi, T. Sampei and A. Tomiyama, Study on flows inside and outside an air diffuser for membrane bioreactor, *Journal of Fluid Science and Technology*, 7, pp.78-88, 2012.
- [12] H. Fan, L. Qi, G. Liu, Y. Zhang, Q. Fan, H. Wang, Aeration optimization through operation at low dissolved oxygen concentrations: Evaluation of oxygen mass transfer dynamics in different activated sludge systems, *Journal of Environmental Sciences*, 55, pp. 224-235, 2017.
- [13] K. Mishima and M. Ishii, Theoretical prediction of onset of horizontal slug flow, *Journal of Fluids Engineering*, 102, pp. 441-445, 1980.